Nuclear Physics B (Proc. Suppl.) 37B (1994) 181–192
North-Holland

NUCLEAR PHYSICS B
PROCEEDINGS
SUPPLEMENTS

Leptoquark Production at High Energy e^+e^- Colliders

J. Blümlein[a] and E. Boos*[b]

[a]DESY–Zeuthen, Platanenallee 6, D–15735 Zeuthen, Germany

[b]Department of Nuclear Physics, Moscow State University, RU–119899 Moscow, Russia

The prospects to search for scalar and vector leptoquarks at high energy e^+e^- colliders are reviewed. We compare production cross sections in the energy range between $\sqrt{s} = \mathcal{O}(200\,\mathrm{GeV})$ and 1 TeV for e^+e^- annihilation. QED and QCD corrections and the effect of beamstrahlung in these processes are discussed. For the case of linear colliders the search potential in the different possible collider modes as e^+e^- annihilation, $e^\pm\gamma$ scattering, and $\gamma\gamma$ fusion is compared.

1. Introduction

Leptoquark states emerge in various extensions of the Standard Model both in Grand Unified Theories and scenarios of fermion compositeness [1]. One may claim a more fundamental reason behind the observed tight correlation of lepton and quark quantum numbers in the $SU(2)_L \times U(1)_Y$ theory, which leads to anomaly cancellation and may be related to fields carrying both lepton and quark quantum numbers.

Severe constraints have been derived on the fermion couplings of leptoquarks during the last years in the analysis of rare decays [2] and studies of electron–quark scattering at high energies [3]. Because these couplings are generally not predicted in the individual models experimental searches have to always limit both these parameters and the particle mass.

Conversely, one may study production mechanisms, e.g. pair production, involving only the couplings of leptoquarks to gauge bosons being known in the Standard Model. The phase space is smaller but a *decisive* search for these states is possible. The recent analysis of leptoquark pair production in e^+e^- annihilation [4, 5] at LEP [6] has led to a thorough exclusion of leptoquarks of all families in the mass range up to $\sim 45\,\mathrm{GeV}$. Large pair production cross sections are also obtained in $p\bar{p}$ and pp scattering [7, 8]. However, since leptoquarks are either color triplets or antitriplets other interactions are needed to determine their flavour, charge, and weak coupling quantum numbers, as well as possible anomalous couplings in the case of vector leptoquarks. These quantum numbers can be disentangeled studying their production and decay at e^+e^- or ep [9] colliders.

An extension of the mass range will be obtained by LEP200 for leptoquarks of any family. High energy linear colliders in the energy range from $\sqrt{s} = 500\,\mathrm{GeV}$ to $1\,\mathrm{TeV}$ will extend the range further and, moreover, allow to study $e\gamma$ and $\gamma\gamma$ scattering as complementary options at similar luminosities[2].

In this paper we review the prospects to search for both scalar and vector leptoquarks in e^+e^- annihilation, $e\gamma$ scattering and $\gamma\gamma$ fusion at future high energy colliders. For definiteness we consider the class of leptoquarks containing dimensionless couplings to fermions, which are baryon and lepton number conserving, family diagonal, and respect $SU(3)_c \times SU(2)_L \times U(1)_Y$ symmetry. The leptoquark states obeying these properties have been introduced in [11].

The paper is organized as follows. In section 2 the Lagrangians of these leptoquark states for fermion interactions and interactions with gauge bosons are given and their quantum numbers are summarized. In section 3 pair production of leptoquarks in e^+e^- annihilation is considered. As known from other processes [12], the QED radiative corrections for pair production at threshold – a typical situation in the search for new

*Supported by Ministry for Science, Research, and Culture of Land Brandenburg, contract II. 1-3141-2/8(94).

[2]The possibility to produce leptoquarks in e^-e^- [10] collisions has also been studied recently.

SSDI 0920-5632(94)00627-X

particles – may be rather large. Effects due to beamstrahlung at linear colliders are substantial in this range. Furthermore, sizeable QCD final state corrections are expected [13]. These aspects are dealt with in section 4. Single leptoquark production in e^+e^- and $e\gamma$ scattering is considered section 5. Pair production in $\gamma\gamma$ fusion is dealt with in section 6. Section 7 contains a comparison of the different collider options.

2. Classification of Leptoquark States

There exist nine scalar and nine vector leptoquark states carrying $SU(3)_c \times SU(2)_L \times U(1)_Y$ invariant couplings, which are B and L conserving and family diagonal [11]. The effective Lagrangian which describes their interaction with fermions and neutral gauge bosons in the low energy range ($M_\Phi \lesssim 1\,\mathrm{TeV}$) is given by

$$\mathcal{L} = \mathcal{L}^f_{|F|=2} + \mathcal{L}^f_{F=0} + \mathcal{L}^{\gamma,Z,g} + \mathcal{L}^v_{an} \tag{1}$$

with

$$\begin{aligned}\mathcal{L}^f_{|F|=2} &= (g_{1L}\bar{q}^c_L i\tau_2 l_L + g_{1R}\bar{u}^c_R e_R)S_1 \\ &+ \tilde{g}_{1R}\bar{d}^c_R e_R \tilde{S}_1 + g_{3L}\bar{q}^c_L i\tau_2 \vec{\tau} l_L \vec{S}_3 \\ &+ (g_{2L}\bar{d}^c_R \gamma^\mu l_L + g_{2R}\bar{q}^c_L \gamma^\mu e_R)V_{2\mu} \\ &+ \tilde{g}_{2L}\bar{u}^c_R \gamma^\mu l_L \tilde{V}_{2\mu} + h.c.,\end{aligned} \tag{2}$$

$$\begin{aligned}\mathcal{L}^f_{F=0} &= (h_{2L}\bar{u}_R l_L + h_{2R}\bar{q}_L i\tau_2 e_R)R_2 \\ &+ \tilde{h}_{2L}\bar{d}_R l_L \tilde{R}_2 + (h_{1L}\bar{q}_L \gamma^\mu l_L \\ &+ h_{1R}\bar{d}_R \gamma^\mu e_R)U_{1\mu} + \tilde{h}_{1R}\bar{u}_R \gamma^\mu e_R \tilde{U}_{1\mu} \\ &+ h_{3L}\bar{q}_L \vec{\tau}\gamma^\mu l_L \vec{U}_{3\mu} + h.c.\end{aligned} \tag{3}$$

where $F = 3B + L$ and

$$\begin{aligned}\mathcal{L}^{\gamma,Z,g} &= \sum_{scalars} [(D^\mu \Phi)^\dagger (D_\mu \Phi) - M^2 \Phi^\dagger \Phi] \\ &+ \sum_{vectors} \left[-\frac{1}{2} G^\dagger_{\mu\nu} G^{\mu\nu} + M^2 \Phi^{\mu\dagger} \Phi_\mu\right]\end{aligned} \tag{4}$$

In (4) only the *minimal* vector leptoquark couplings are described. Notation for the leptoquarks follows ref. [11]. The covariant derivative is

$$D_\mu = \partial_\mu - ieQ^\gamma A_\mu - ieQ^Z Z_\mu - ig_s \frac{\lambda_a}{2}\mathcal{A}^a_\mu \tag{5}$$

where A_μ, Z_μ and $\mathcal{A}_\mu$ denote the photon–, Z–boson, and gluon fields, respectively, and $G_{\mu\nu} = D_\mu \Phi_\nu - D_\nu \Phi_\mu$ is the field strength tensor. $Q^\gamma = Q_{em}$ denotes the electromagnetic charge of a given leptoquark, $Q^Z = (T_3 - Q_{em}\sin^2\theta_w)/\cos\theta_w \sin\theta_w$, with T_3 the third component of the weak isospin and θ_w the weak mixing angle, g_s is the strong coupling constant and λ_a are the Gell–Mann matrices. Note, that the triple boson couplings appearing in (4) for vector leptoquarks are *not* gauge couplings. For the case of the photon–vector leptoquark interaction the anomalous (*non–minimal*) terms are

$$\mathcal{L}^\gamma_{an} = -ie\left[(1-\kappa_A)\Phi^\dagger_\mu \Phi_\nu F^{\mu\nu} + \frac{\lambda_A}{M_v^2} G^\dagger_{\sigma\mu} G^\mu_\nu F^{\nu\sigma}\right] \tag{6}$$

The Lagranian (1) is $U_{em}(1)$ invariant. The anomalous couplings κ_A and λ_A are related to the QED anomalous magnetic moment μ_Φ and electric quadrupole moment q_Φ of leptoquarks by

$$\begin{aligned}\mu_{\Phi,A} &= \frac{eQ_\gamma}{2M_\Phi}(2 - \kappa_A + \lambda_A) \\ q_{\Phi,A} &= -\frac{eQ_\gamma}{M^2_\Phi}(1 - \kappa_A - \lambda_A)\end{aligned} \tag{7}$$

The quantum numbers of the different leptoquark states are summarized in table 1.

3. Pair Production in e^+e^- Annihilation

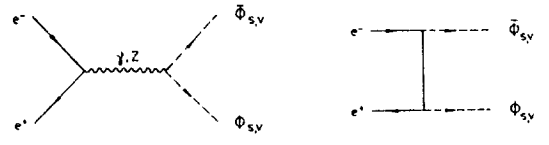

Fig. 1 Born diagrams for leptoquark pair production in e^+e^- annihilation

The integrated production cross section for scalar[4, 5] and vector leptoquarks are [4]

$$\begin{aligned}\sigma_s(s) = \frac{\pi\alpha^2\beta^3}{2s}\sum_{a=L,R}\Big\{&|\kappa_a(s)|^2 \\ &+ \left(\frac{\lambda_a}{e}\right)^2 Re[\kappa_a(s)]F_1(\beta) + \left(\frac{\lambda_a}{e}\right)^4 F_2(\beta)\Big\}\end{aligned} \tag{8}$$

Tab. 1 Quantum numbers of leptoquarks [4].

leptoquark (Φ)	spin	F	colour	T_3	Q_{em}	$\lambda_L(lq)$	$\lambda_R(lq)$	$\lambda_L(\nu q)$
S_1	0	-2	$\bar{3}$	0	1/3	g_{1L}	g_{1R}	$-g_{1L}$
$\tilde{S}_1$	0	-2	$\bar{3}$	0	4/3	0	$\tilde{g}_{1R}$	0
$\vec{S}_3$	0	-2	$\bar{3}$	$+1$	4/3	$-\sqrt{2}g_{3L}$	0	0
				0	1/3	$-g_{3L}$	0	$-g_{3L}$
				-1	$-2/3$	0	0	$\sqrt{2}g_{3L}$
R_2	0	0	3	1/2	5/3	h_{2L}	h_{2R}	0
				$-1/2$	2/3	0	$-h_{2R}$	h_{2L}
$\tilde{R}_2$	0	0	3	1/2	2/3	$\tilde{h}_{2L}$	0	0
				$-1/2$	$-1/3$	0	0	$\tilde{h}_{2L}$
$V_{2\mu}$	1	-2	$\bar{3}$	1/2	4/3	g_{2L}	g_{2R}	0
				$-1/2$	1/3	0	g_{2R}	g_{2L}
$\tilde{V}_{2\mu}$	1	-2	$\bar{3}$	1/2	1/3	$\tilde{g}_{2L}$	0	0
				$-1/2$	$-2/3$	0	0	$\tilde{g}_{2L}$
$U_{1\mu}$	1	0	3	0	2/3	h_{1L}	h_{1R}	h_{1L}
$\tilde{U}_{1\mu}$	1	0	3	0	5/3	0	$\tilde{h}_{1R}$	0
$\vec{U}_{3\mu}$	1	0	3	$+1$	5/3	$\sqrt{2}h_{3L}$	0	0
				0	2/3	$-h_{3L}$	0	h_{3L}
				-1	$-1/3$	0	0	$\sqrt{2}h_{3L}$

Tab. 2 Branching ratios for final states arrising from the decays of leptoquarks associated with the first ($l = e$) and second ($l = \mu$) family. The sequence of branching fractions given in the second and third row refers to the assumptions $\lambda_L = \lambda_R, \lambda_L = 0$, and $\lambda_R = 0$, respectively [4].

states	$l^+l^- + 2jets$	$l\nu + 2jets$	$\nu\bar{\nu} + 2jets$
S_1 U_1	$\frac{4}{9}$ 1 $\frac{1}{4}$	$\frac{4}{9}$ 0 $\frac{1}{2}$	$\frac{1}{9}$ 0 $\frac{1}{4}$
$R_2^{2/3}$ $V_2^{1/3}$	$\frac{1}{4}$ 1 0	$\frac{1}{2}$ 0 0	$\frac{1}{4}$ 0 1
$S_3^{1/3}$ $U_3^{2/3}$	$\frac{1}{4}$	$\frac{1}{2}$	$\frac{1}{4}$
$\tilde{S}_1$ $S_3^{4/3}$ $R_2^{5/3}$ $\tilde{R}_2^{2/3}$ $V_2^{4/3}$ $\tilde{V}_2^{1/3}$ $\tilde{U}_1$ $U_3^{5/3}$	1	0	0
$S_3^{-2/3}$ $\tilde{R}_2^{-1/3}$ $\tilde{V}_2^{-2/3}$ $U_3^{-1/3}$	0	0	1

$$\sigma_v(s) = \frac{\pi\alpha^2\beta}{2M_\Phi^2}\sum_{a=L,R}\left\{|\kappa_a(s)|^2\tilde{F}_1(\beta) + \left(\frac{\lambda_a}{e}\right)^2 Re[\kappa_a(s)]\tilde{F}_2(\beta) + \left(\frac{\lambda_a}{e}\right)^4\tilde{F}_3(\beta)\right\}. \quad (9)$$

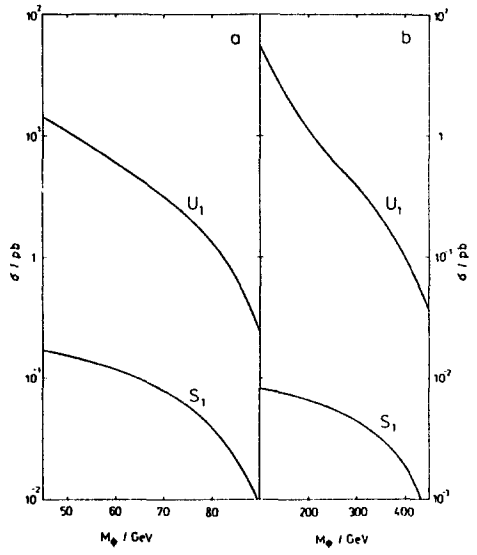

Fig. 2 The pair production cross sections for the leptoquarks S_1 and U_1 for a) $\sqrt{s} = 190\,\text{GeV}$ and b) $\sqrt{s} = 1\,\text{TeV}$ [4].

The corresponding diagrams are shown in figure 1. The cross sections are the same for $F = 0$ and $|F| = 2$ type leptoquarks since the fermions entering the process are treated as massless. In the above,

$$\kappa_a(s) = \sum_{V=\gamma,Z} Q_a^V(e)\frac{s}{s - M_V^2 + iM_V\Gamma_V}Q^V(\Phi), \quad (10)$$

where $Q_{L,R}^\gamma(e) = -1$, $Q_L^Z(e) = (-1/2 + \sin^2\theta_w)/\cos\theta_w\sin\theta_w$, and $Q_R^Z(e) = \tan\theta_w$ are the relevant charges for the electron. M_V and Γ_V denote the mass and the width of the neutral current gauge bosons. Furthermore, $\beta = \sqrt{1 - 4M_\Phi^2/s}$ and the functions $F_i(\beta)$ and $\tilde{F}_i(\beta)$ are

$$F_1(\beta) = \frac{3}{2}\left(\frac{1+\beta^2}{\beta^2} - \frac{(1-\beta^2)^2}{2\beta^3}\ln\frac{1+\beta}{1-\beta}\right) \quad (11)$$

$$F_2(\beta) = 3\left(-\frac{1}{\beta^2} + \frac{1+\beta^2}{2\beta^3}\ln\frac{1+\beta}{1-\beta}\right) \quad (12)$$

$$\tilde{F}_1(\beta) = \beta^2\left(\frac{7-3\beta^2}{4}\right) \quad (13)$$

$$\tilde{F}_2(\beta) = \frac{15}{4} + 2\beta^2 - \frac{3}{4}\beta^4 - \frac{3}{8\beta}(1-\beta^2)^2(5-\beta^2)\ln\frac{1+\beta}{1-\beta} \quad (14)$$

$$\tilde{F}_3(\beta) = 3(1+\beta^2) + \frac{\beta^2}{4}\frac{s}{M_\Phi^2} + \frac{3}{2\beta}(1-\beta^4)\ln\frac{1+\beta}{1-\beta}. \quad (15)$$

The differential distributions were given in [4].

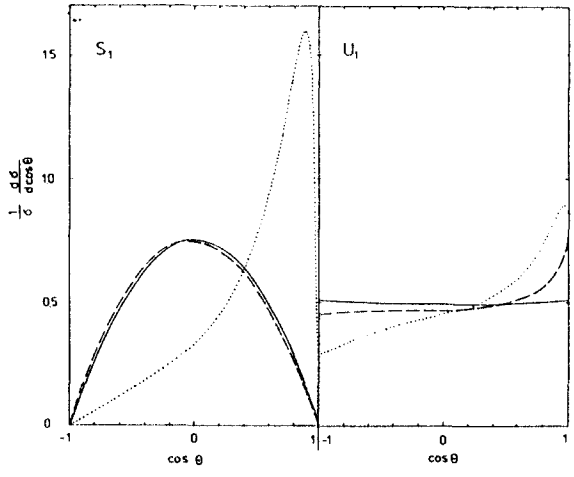

Fig. 3 Angular distributions for leptoquark pair production at $\sqrt{s} = 1\,\text{TeV}$. Full line $\lambda_{L,R} = 0$; dashed line $\lambda_L/e = 0.3, \lambda_R = 0$; dotted line: $\lambda_R/e = 1$, $\lambda_L = 0$ [4].

Asymptotically, for $s \gg M_Z^2, M_\Phi^2$, the cross sections for scalar leptoquark production behave like $\sim \ln(s/M_\Phi^2)/s$. In the case of vector leptoquarks[3] with *minimal* coupling to the photon and Z–boson the pure s–channel contribution and the interference of the s– and t–channel terms approach a finite value *contrary* to the case of gauge

[3] In [14] the pair production of vector leptoquarks of the type [15] is discussed assuming Yang–Mills type couplings and very large fermion couplings $\lambda/e = 1/\sqrt{\sin^2\theta_w} \approx 2.09$ which are linked to the gauge couplings to obtain tree–level unitarity.

couplings. The pure t–channel contribution grows proportional to s, however. There is *no* genuine relation between the fermion and gauge boson couplings for leptoquarks in general. The effective Lagrangian (1) is assumed to describe the leptoquark interactions in the low energy range $s/M_\Phi^2 \leq 1$ only and has to be supplemented by other terms provided by the respective underlying theory at high energies which restore unitarity. For the leptoquarks S_1 and U_1 the production cross sections are the lowest among the scalar and vector leptoquarks, respectively. Assuming an integrated luminosity of $\mathcal{L} = 500$ pb^{-1} for LEP200 and $\mathcal{L} = 10$ fb^{-1} for a 1 TeV linear collider one can reach search limits assuming 50 signal events of about 70 GeV and 250 GeV for the state S_1 at LEP200 and a 1 TeV collider, respectively, whereas all vector leptoquark states can be searched for up to the kinematical limit practically (figure 2). Figure 3 shows that the spin of the produced leptoquarks can be clearly determined from the cms angular distribution in e^+e^- annihilation.

4. Radiative Corrections to e^+e^- Annihilation

4.1. QED Initial State Corrections

The dominant contributions to the QED corrections are due to the initial state corrections. In [13] these terms have been calculated in leading order up to $\mathcal{O}(\alpha^2)$ including also soft photon exponentiation.

$$\Delta\sigma_{tot}^{QED,is}(s) = \sigma_{tot}^{(1,\gamma)}(s) + \sigma_{tot}^{(2,2\gamma)}(s) + \sigma_{tot}^{(2,e\gamma e)}(s) + \sigma_{tot}^{(2,f\bar{f})}(s) + \sigma_{tot}^{(>2,soft)}(s) \quad (16)$$

Each term can be expressed as convolutions of a splitting function and the Born cross sections.

$$\sigma_{tot}^{(i,X)} = \left(\frac{\alpha}{\pi}L_m\right)^i \int_0^1 dz P_X(z) \left[\sigma_{tot}^{(0)}(zs) \times \theta\left(z - \frac{4M_\Phi^2}{s}\right) - C_X\sigma_{tot}^{(0)}(s)\right] \quad (17)$$

with $L_m = \log(s/m^2)$ and $C_X = 1$ for bremsstrahlung and $C_X = 0$ otherwise, (cf. [13] for details). The contributions are due to single and double photon bremsstrahlung and e^+e^- and fermion pair ($f\bar{f}$) production. While the latter terms amount to a few per cent only [13] the bremsstrahlung contributions are large in the threshold range.

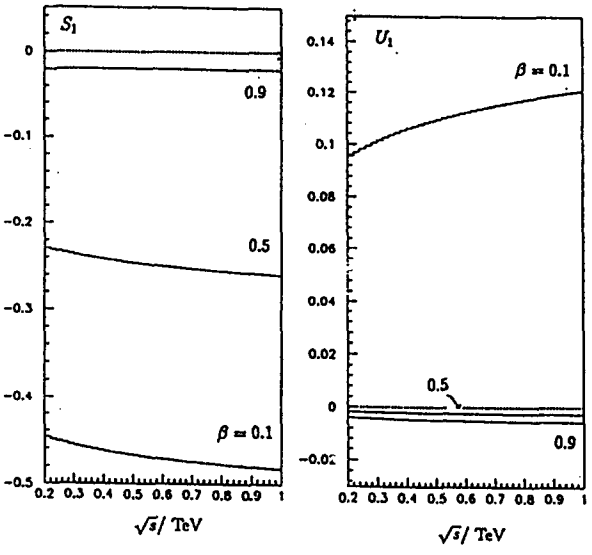

Fig. 4 QED initial state bremsstrahlung corrections for $e^+e^- \to \Phi\bar{\Phi}$; a) leading order terms up to $\mathcal{O}(\alpha^2)$ + soft exponentiation for scalar leptoquarks; b) $\mathcal{O}(\alpha^2)$ + soft exponentiation terms only for vector leptoquarks [13].

In figure 4a the bremsstrahlung corrections are illustrated for scalar leptoquark pair production and amount to -45% at $\beta = 0.1$. Figure 4b shows the correction excluding the $\mathcal{O}(\alpha)$ term. The 2nd and higher order corrections are positive and amount to about 10 % of the Born cross section.

4.2. Beamstrahlung

The effect of beamstrahlung has a significant impact on production cross sections at high energy linear colliders [16]. Numerical studies have been performed for a series of accelerators [17]. The beamstrahlung correction can be described by the convolution

$$\Delta\sigma_{BS}(s) = \int_0^1 dz \frac{1}{\mathcal{L}}\frac{d\mathcal{L}}{dz}(z)\sigma^{(0)}(zs) \times \theta\left(z - \frac{4M^2}{s}\right) - \sigma^{(0)}(s). \quad (18)$$

The normalized longitudinal luminosity distribution $(1/\mathcal{L})d\mathcal{L}(z)/dz$ has to be determined by Monte Carlo simulations of the accelerator type considered. In figure 5 the beamstrahlung correction to the production cross section for scalar and vector leptoquarks is shown using a simulated spectrum $(1/\mathcal{L})d\mathcal{L}(z)/dz$ [18] for $\sqrt{s} = 300$ GeV. Although a spectrum for a narrow band machine has been considered the corrections amount to $\mathcal{O}(-80\ \%)$ for $\beta \approx 0.1$.

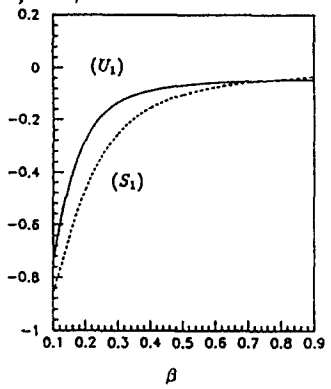

Fig. 5 Beamstrahlung correction for the leptoquark pair production cross section of S_1 and U_1 for a narrow band machine at $\sqrt{s} = 300$ GeV as a function of β [13].

4.3. QCD Corrections

For small fermionic couplings $\lambda_{L,R}/e \ll 1$ the final state QCD and QED corrections are described by a single form factor $\mathcal{F}_s(\beta)$ for scalar[4] leptoquarks [19] given by

$$\begin{aligned}\mathcal{F}_s(\beta) &= \left[4\mathrm{Li}_2\left(\frac{1-\beta}{1+\beta}\right) + 2\mathrm{Li}_2\left(-\frac{1-\beta}{1+\beta}\right)\right. \\ &- \left. 3\ln\frac{2}{1+\beta}\ln\frac{1+\beta}{1-\beta} - 2\ln\beta\ln\frac{1+\beta}{1-\beta}\right] \\ &\times \frac{1+\beta^2}{\beta} - 3\ln\left(\frac{4}{1-\beta^2}\right) - 4\ln\beta \\ &+ \frac{1}{\beta^3}\left[\frac{5(1+\beta^2)^2}{4} - 2\right]\ln\frac{1+\beta}{1-\beta} \\ &+ \frac{3}{2}\frac{1+\beta^2}{\beta^2} \qquad (19)\end{aligned}$$

[4] For vector leptoquarks QCD corrections can only be calculated in the standard way in the case $\kappa_g = \lambda_g = 0$. For other values of these couplings the Lagrangian has to be supplemented by higher order operators to absorb divergent terms.

Here, $\mathrm{Li}_2(x) = -\int_0^x dt \ln(1-t)/t$ denotes the dilogartithm. The final state corrections are $\delta_{fs} = 1 + C(\alpha_s/\pi)\mathcal{F}_s(\beta)$ are shown in figure 6 where $C = C_F = 4/3$, $\alpha = \alpha_s$ for QCD and $C = 1$, $\alpha = \alpha_{QED}$ for QED. The form factor is dominated by π^2-terms and peaks at low β due to the Coulomb singularity which indicates the onset of possible bound state creation. The QCD corrections are always larger than $\sim 40\%$. Thus the QCD corrections compensate for the lowering of the cross section due to the initial state QED radiation and beamstrahlung.

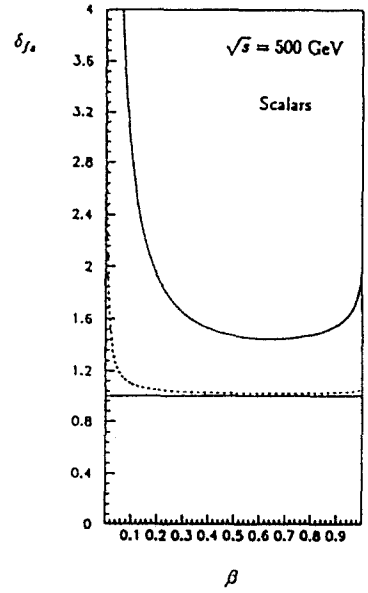

Fig. 6 1st order final state corrections δ_{fs} for scalar leptoquark pair production for e^+e^- annihilation vs β. Full line: QCD corrections, dotted line QED corrections [13].

Formation of Bound States

The Coulomb singularity of the QCD corrections for $\beta \to 0$ accounts for possible bound state formation of the $\Phi\bar{\Phi}$ pair[5]. Both the e^+e^- annihilation cross sections for scalar and vector leptoquarks behave for small β like

$$\begin{aligned}\sigma(e^+e^- \to \Phi_s\bar{\Phi}_s) &\propto \beta^3 \\ \sigma(e^+e^- \to \Phi_v\bar{\Phi}_v) &\propto \beta^3 \qquad (20)\end{aligned}$$

[5] In the case of scalars this is identical to stoponium formation [20, 13].

while for $\gamma\gamma$ fusion the behaviour is

$$\begin{aligned}\sigma(\gamma\gamma \to \Phi_s\overline{\Phi}_s) &\propto \beta \\ \sigma(\gamma\gamma \to \Phi_v\overline{\Phi}_v) &\propto \beta\end{aligned} \tag{21}$$

cf. (8,9) and (25,27). The chance to find possible bound states is thus larger in $\gamma\gamma$ fusion than in e^+e^- annihilation.

5. $e^\pm\gamma$ Scattering

5.1. Single Leptoquark Production in e^+e^- annihilation

The production cross sections for single leptoquark production is proportional to $(\lambda_{L,R}/e)^2$ and thus sensitive to the unpredicted leptoquark fermion couplings. In the subsequent illustrations we will always assume $\lambda/e \equiv 1$ and concentrate on the sensitivity of the different observables with respect to the particle mass.

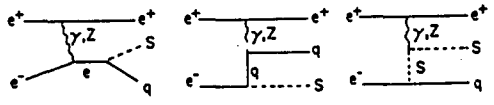

Fig. 7 Dominant diagrams for single leptoquark production in e^+e^- scattering.

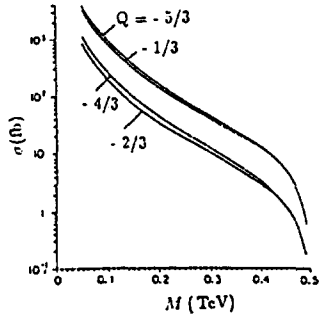

Fig. 8 Direct contribution to the cross section for single leptoquark production in e^+e^- scattering at $\sqrt{s} =$ 500 GeV for scalar leptoquarks with $\lambda/e = 1$ [21].

Single production of scalar leptoquarks in e^+e^- annihilation has been studied in [21] for the case of direct production. The dominant diagrams are shown in figure 7. In principle, family two and three leptoquarks can be produced in e^+e^- annihilation but the production cross section is much smaller than that for the first family. As seen in figure 8, masses nearly as large as the kinematical limit are accessible for all scalar leptoquarks with $\lambda/e \equiv 1$ at a 500 GeV linear collider assuming a signal of 50 events. The resolved photon terms are also important. They have been studied in [22] for scalar leptoquark production. The photon beam spectrum is assumed to be described by the Williams Weizsäcker approximation (WWA) and different parametrizations of parton distributions in the photon have been compared. Figure 9 shows the production cross sections as a function of the leptoquark mass and charge. Again the cross section is so large that nearly the whole kinematical range can be probed if $\lambda = e$.

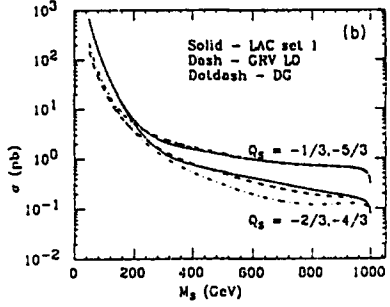

Fig. 9 Resolved photon contribution $\gamma^*e \to q\bar{q} + e \to Sq$ for single scalar leptoquark production for $\lambda/e = 1$ at $\sqrt{s} = 1$ TeV [22]. The photon distribution is calculated in WWA.

5.2. Single Leptoquark Production in $e\gamma$ Compton Scattering

The production of leptoquarks in $e\gamma$ scattering can be studied directly at high energy linear colliders by converting one of the electron beams into a photon beam through Compton back scattering of a Laser beam [23]. The resulting photon spectrum is

$$\begin{aligned}\Phi_\gamma(z) &= \frac{1}{N(x)}\left[1 - z + \frac{1}{1-z} - \frac{4z}{x(1-z)}\right. \\ &+ \left.\frac{4z^2}{x^2(1-z)^2}\right]\end{aligned} \tag{22}$$

with the normalization

$$\begin{aligned}N(x) &= \frac{16 + 32x + 18x^2 + x^3}{2x(1+x)^2} \\ &+ \frac{x^2 - 4x - 8}{x^2}\ln(1+x),\end{aligned} \tag{23}$$

where $z \leq z_{max} = x/(x+1) \equiv 2(\sqrt{2}+1)/(2\sqrt{2}+3)$ is given by the pair production threshold.

Single production of scalar leptoquarks via $e\gamma \to S\overline{q}$ has been studied first in [24].

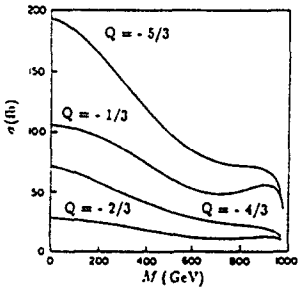

Fig. 10 Direct contribution to the $e\gamma$ scattering cross section for scalar leptoquarks at $\sqrt{s} = 1$ TeV for a real photon beam ($d\mathcal{L}/dz = \delta(1-z)$) with $\lambda/e = 1$ [25].

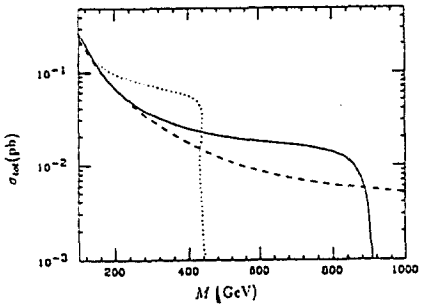

Fig. 11 Integrated cross section of scalar leptoquark production $e\gamma \to S\overline{u}$ in Laser backscattering. The contribution due to $eg_\gamma \to S\overline{u}$ is added. Dashed line: $\sqrt{s} = 2$ TeV, full line: $\sqrt{s} = 1$ TeV, dotted line: $\sqrt{s} = 500$ GeV [26].

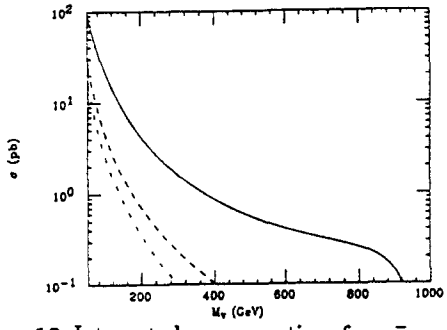

Fig. 12 Integrated cross section for $e^-\gamma \to \Phi_v q$ vs M_v for $\lambda/e \approx 2.09$. Full line: Compton Laser $\sqrt{s} = 1$ TeV; dotted line: $\sqrt{s} = 500$ GeV; dashed line: WWA $\sqrt{s} = 1$ TeV; dash-dotted line: $\sqrt{s} = 500$ GeV [14].

The production cross section for scalar leptoquarks was invesigated in [25] in the energy range of future linear colliders. In figure 10 the mass dependence of the production cross section for the different leptoquark types is shown. The cross sections are large enough to allow for a search in almost the full kinematical range.

In [26] the production of scalar leptoquarks of the type discussed in [15] are studied referring to the Compton photon spectrum. The resolved photon contributions due to $eg_\gamma \to S\overline{u}$ are added to the direct terms. At a signal level of 50 events the accessible mass range is found to extend to about $0.45\sqrt{s}$ (figure 11).

The single production of vector leptoquarks of the type [15] was studied in [14] again assuming Yang–Mills type couplings of the photon to the leptoquark. The cross sections are much larger than in the case of scalar leptoquarks. Different options are compared in figure 12. It is also shown that the production cross sections are larger by orders of magnitude in the high mass range for $e\gamma$ scattering in the case of a Compton photon spectrum compared to the WWA spectrum.

6. Pair Production in $\gamma\gamma$ Scattering

6.1. Scalar Leptoquarks

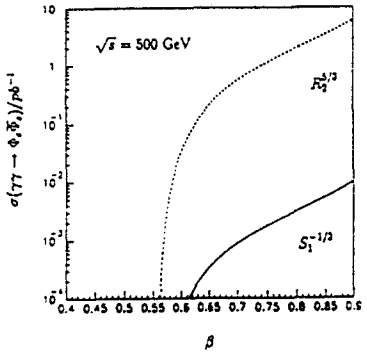

Fig. 13 Integrated cross section for the pair production of scalar leptoquarks in $\gamma\gamma$ fusion vs β [13].

The differential and integral production cross sections are well-known [27] and given by

$$\frac{d\hat{\sigma}_s}{d\cos\theta} = \frac{\pi\alpha^2}{\hat{s}} Q_\Phi^4 N_c \beta \left\{ 1 - \frac{2(1-\beta^2)}{1-\beta^2\cos^2\theta} + \frac{2(1-\beta^2)^2}{(1-\beta^2\cos^2\theta)^2} \right\} \qquad (24)$$

and

$$\hat{\sigma}_s(\hat{s},\beta) = \frac{\pi\alpha^2}{\hat{s}} Q_\Phi^4 N_c \left\{ 2(2-\beta^2)\beta - (1-\beta^4)\log\left|\frac{1+\beta}{1-\beta}\right| \right\} \quad (25)$$

where $N_c = 3$. Numerical results have been derived for the case of a $\gamma\gamma$ collider operating at $\sqrt{s} = 500\,\mathrm{GeV}$ in [13]. As seen in figure 13 only leptoquarks with large charges can be pair produced at a sufficient rate in this reaction.

In [21] single production of scalar leptoquarks is considered for $\gamma\gamma$ fusion via $\gamma\gamma \to \bar{l}qS$. At typical luminosities the search limits reach 0.8 to $0.9\sqrt{s}$ for M_s.

6.2. Vector Leptoquarks

The differential and integral production cross section for vector leptoquarks are

$$\frac{d\hat{\sigma}_v}{d\cos\theta} = \frac{\pi\alpha^2}{\hat{s}} Q_\Phi^4 N_c \sum_{j=0}^{14} \chi_j \frac{F_j(\hat{s},\beta,\cos\theta)}{(1-\beta^2\cos^2\theta)^2} \quad (26)$$

with $\chi_j = \chi_j(\kappa_A, \lambda_A)$ and

$$\begin{aligned}\sum_{j=0}^{14}\chi_j F_j &= F_0 + \kappa_A F_1 \\ &+\kappa_A^2 F_2 + \kappa_A^3 F_3 + \kappa_A^4 F_4 \\ &+\lambda_A F_5 + \lambda_A^2 F_6 + \lambda_A^3 F_7 \\ &+\lambda_A^4 F_8 + \kappa_A\lambda_A F_9 + \kappa_A\lambda_A^2 F_{10} \\ &+\kappa_A\lambda_A^3 F_{11} + \kappa_A^2\lambda_A F_{12} + \kappa_A^3\lambda_A F_{13} \\ &+\kappa_A^2\lambda_A^2 F_{14}\end{aligned}$$

and

$$\hat{\sigma}_v = \frac{2\pi\alpha^2}{M_v^2} Q_\Phi^4 N_c \sum_{j=0}^{14} \chi_j(\kappa_A,\lambda_A)\tilde{F}_j(\hat{s},\beta) \quad (27)$$

with

$$\tilde{F}_j = \frac{M_v^2}{\hat{s}} \int_0^\beta d\xi \frac{F_j(\xi = \beta\cos\theta)}{(1-\xi^2)^2} \quad (28)$$

Eq. (26) agrees analytically with a result obtained in [28]. The functions $F_j(\hat{s},\beta,\cos\theta)$ are not given here but can be obtained as linear combinations from relations given in eqs. (12,13) and (17) in [9].

$$\begin{aligned}\tilde{F}_0 &= \beta\left(\frac{11}{2} - \frac{9}{4}\beta^2 + \frac{3}{4}\beta^4\right) \\ &- \frac{3}{8}\left(1-\beta^2-\beta^4+\beta^6\right)\ln\left|\frac{1+\beta}{1-\beta}\right| \\ \tilde{F}_1 &= -8\beta - \frac{3}{2}\left(1-\beta^2\right)\log\left|\frac{1+\beta}{1-\beta}\right| \\ \tilde{F}_2 &= 3\beta + \frac{1}{4}\beta\frac{\hat{s}}{M_\Phi^2} + \left(\frac{7}{2} - 2\beta^2\right)\log\left|\frac{1+\beta}{1-\beta}\right| \\ \tilde{F}_3 &= -\frac{1}{4}\beta\frac{\hat{s}}{M_\Phi^2} + \left(-2 + \frac{3}{4}\beta^2\right)\log\left|\frac{1+\beta}{1-\beta}\right| \\ \tilde{F}_4 &= -\frac{1}{96}\beta + \frac{5}{48}\beta\frac{\hat{s}}{M_\Phi^2} + \frac{4-\beta^2}{16}\log\left|\frac{1+\beta}{1-\beta}\right| \\ \tilde{F}_5 &= -\left(1-\beta^2\right)\log\left|\frac{1+\beta}{1-\beta}\right| \\ \tilde{F}_6 &= -\frac{1}{6}\beta + \frac{17}{12}\beta\frac{\hat{s}}{M_\Phi^2} \\ &+ \left(-3 - \frac{\beta^2}{2} + \frac{1}{2}\frac{\hat{s}}{M_\Phi^2}\right)\log\left|\frac{1+\beta}{1-\beta}\right| \\ \tilde{F}_7 &= -\beta + \frac{11}{6}\beta\frac{\hat{s}}{M_\Phi^2} - \frac{1}{3}\beta\frac{\hat{s}^2}{M_\Phi^4} \\ &- \frac{3+\beta^2}{4}\log\left|\frac{1+\beta}{1-\beta}\right| \\ \tilde{F}_8 &= -\frac{1}{96}\beta + \frac{59}{80}\beta\frac{\hat{s}}{M_\Phi^2} - \frac{113}{320}\beta\frac{\hat{s}^2}{M_\Phi^4} + \frac{43}{960}\beta\frac{\hat{s}^3}{M_\Phi^6} \\ &+ \left(-\frac{1}{2} - \frac{1}{16}\beta^2 + \frac{1}{8}\frac{\hat{s}}{M_\Phi^2}\right)\log\left|\frac{1+\beta}{1-\beta}\right| \\ \tilde{F}_9 &= 2\beta + (2+\beta^2)\log\left|\frac{1+\beta}{1-\beta}\right| \\ \tilde{F}_{10} &= 2\beta - \frac{7}{3}\beta\frac{\hat{s}}{M_\Phi^2} \\ &+ \left(3 + \frac{5}{4}\beta^2 - \frac{1}{2}\frac{\hat{s}}{M_\Phi^2}\right)\log\left|\frac{1+\beta}{1-\beta}\right| \\ \tilde{F}_{11} &= \frac{1}{24}\beta - \frac{59}{48}\beta\frac{\hat{s}}{M_\Phi^2} + \frac{5}{32}\beta\frac{\hat{s}^2}{M_\Phi^4} \\ &+ \frac{5+\beta^2}{4}\log\left|\frac{1+\beta}{1-\beta}\right| \\ \tilde{F}_{12} &= -\beta - \frac{1}{2}\beta\frac{\hat{s}}{M_\Phi^2} \\ &+ \left(-\frac{1}{4} - \frac{7}{4}\beta^2\right)\log\left|\frac{1+\beta}{1-\beta}\right| \\ \tilde{F}_{13} &= \frac{1}{24}\beta + \frac{1}{3}\beta\frac{\hat{s}}{M_\Phi^2} - \frac{1}{4}\left(1-\beta^2\right)\log\left|\frac{1+\beta}{1-\beta}\right|\end{aligned}$$

$$\tilde{F}_{14} = -\frac{1}{16}\beta + \frac{11}{96}\beta\frac{\hat{s}}{M_\Phi^2} + \frac{17}{192}\beta\frac{\hat{s}^2}{M_\Phi^4} + \left(\frac{1}{8}\frac{\hat{s}}{M_\Phi^2} - \frac{3}{4} - \frac{3}{8}\beta^2\right)\log\left|\frac{1+\beta}{1-\beta}\right| \quad (29)$$

From (27,29) it follows that tree-level unitarity is only obtained for $\lambda_A = 0$ and $\kappa_A^2\left[(\kappa_A - 6/5)^2 + 24/25\right] = 0$, i.e. also $\kappa_A = 0$.

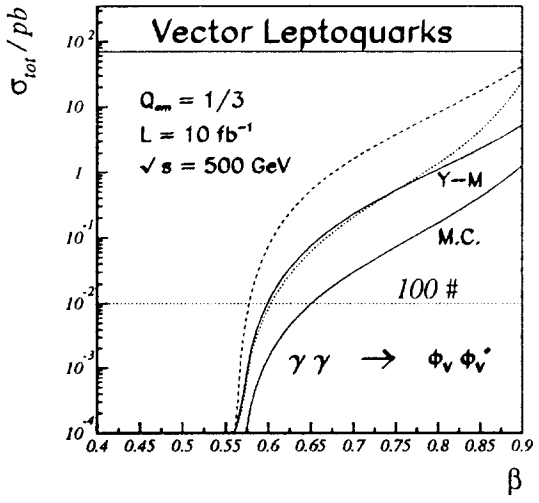

Fig. 14 Vector leptoquark pair production cross section for $\gamma\gamma$ fusion for $Q_{em} = 1/3$ and $\sqrt{s} = 500$ GeV vs β. Full lines: minimum coupling (M.C.) and Yang–Mills (Y–M) coupling; dotted line: $\kappa_A = \lambda_A = 1$; dashed line: $\kappa_A = -1, \lambda_A = 0$.

For other leptoquark types the cross section has to be multiplied by $\times(3Q_{\Phi_v})^4$. The long-known special case $\kappa_A = \lambda_A = 0$ has been studied in [14] also. Even for the lowest charge $|Q_v| = 1/3$ and minimal vector coupling the accessible mass range extends to $\sim 0.4\sqrt{s}$.

7. Current Bounds and the Search Potential at e^+e^- Colliders

An overview on the search potential of the different options at future high energy e^+e^- colliders for leptoquarks is given in table 3 including a comparison with the best current bounds.

Tab. 3 Leptoquark mass bounds from present and for future experiments

Collider	Mass Range	Remarks
LEP		
LQ pairs [6]	> 45 GeV	all LQ's
TEVATRON	> 132 GeV	$\tilde{S}_1, S_3^{4/3}$
LQ pairs[29]		$R_2^{5/3}, \tilde{R}_2^{2/3}$
	> 86 GeV	S_1
		1st family
e^+e^-		
LQ pairs [4]		
LEP 200: S	> 70 GeV	
LEP 200: V	> 90 GeV	(mc vectors)
1 TeV LC: S	> 200 GeV	
1 TeV LC: V	> 500 GeV	(mc vectors)
$\gamma\gamma$		
1 TeV Compton Laser		
LQ pairs: S [13]	> 300 GeV	σ : $\times 1...625$
LQ pairs: V	> 400 GeV	mc vectors
		$\lvert Q_\Phi\rvert = 1/3$
single production [21] : S	> 900 GeV	
$e\gamma$		
single production		
1 TeV LC:		
WWA		
S (dir) [21]	> 900 GeV	$(\lambda/e)^2 = 1$,
S (res) [22]	> 900 GeV	$\propto (\lambda/e)^2$
Compton S [26]	> 900 GeV	$\gamma e \rightarrow \Phi_v q$
Laser : V [14]	> 900 GeV	
HERA eq [3]		
single		1 st family
production: eq :		$(\lambda/e)^2 = 1$
S,V :	$\gtrsim 200$ GeV	$\propto (\lambda/e)^2$
HERA γg [9]		
pair		1 st family
production:		$(\lambda/e)^2 = 1$
dir. S:	> 60 GeV	$\lvert Q_\Phi\rvert = 4/3, 5/3$
dir. V:	$> 55..75$ GeV	mc vectors

We concentrate here on the accessible mass ranges only and fix the fermion couplings $\lambda_{L,R}$.

The different processes discussed offer complementary possibilities to constrain or to measure

the different couplings and quantum numbers of leptoquarks. The $\gamma\gamma$ fusion cross section $\propto Q_\Phi^4$ is most selective concerning the leptoquark charges. The cross sections for ep or Drell–Yan [30] scattering, on the other hand, are $\propto (\lambda_{L,R}/e)^4$ and provide ideal probes of the leptoquark–fermion couplings, as do single leptoquark production in hadron scattering [31]. For vector leptoquarks possible anomalous couplings either to the gluon or the photon fields can be constrained in proton collisions [8] or photon collisions. Pair production in ep collisions [9] is sensitive to both types of anomalous couplings. In principle, also anomalous couplings to the Z boson can be studied in e^+e^- annihilation, however, the cross section is dominated by photon exchange in the high energy range.

Tab. 4
Sensitivity to leptoquark quantum numbers

Scattering Process	LQ	Quantum Numbers
e^+e^-	S,V	$Q_\Phi^\gamma, Q_\Phi^Z, \lambda_{L,R}$
$\gamma\gamma$	S	Q_Φ^γ
	V	$Q_\Phi^\gamma, \kappa_A, \lambda_A$
$e\gamma$	S,V	$\lambda_{L,R}, Q_\Phi^\gamma$
ep	single LQ	$\lambda_{L,R}$
	pairs : S	Q_Φ^γ
	pairs : V	$Q_\Phi^\gamma, \kappa_A, \kappa_G, \lambda_A, \lambda_G$
$p\bar{p}, pp$: pairs	V	κ_G, λ_G $(\lambda_{L,R})$
	S	$(\lambda_{L,R})$
$p\bar{p}, pp$: single production	S,V	$\lambda_{L,R}$

Acknowledgement One of us (E.B.) would like to thank DESY–Zeuthen for the kind hospitality during the stay in which this work has been performed and for financial support by the Land Brandenburg. We would like to thank J. Botts for reading the manuscript.

REFERENCES

1 J.C. Pati and A. Salam, Phys. Rev. **D10** (1974) 275;
E. Farhi and L. Susskind, Phys. Rep. **74** (1981) 277;
L. Lyons, Progr. Part. Nucl. Phys. **10** (1982) 227;
B. Schrempp and F. Schrempp, DESY 84-055; Phys. Lett. **B153** (1985) 101;
J.L. Hewett and T.G. Rizzo, Phys. Rep. **183** (1989) 193;
P.H. Frampton, Mod. Phys. Lett. **A7** (1992) 559.

2 W. Buchmüller and D. Wyler, Phys. Lett. **B177** (1986) 377;
M. Leurer, Phys. Rev. Lett. **71** (1993) 1324; Phys. Rev. **D49** (1994) 333;
S. Davidson, D. Bailey, and B. Campbell, Z. Phys. **C61** (1994) 613.

3 ZEUS Collaboration, M. Derrick et al., Phys. Lett. **B306** (1993) 173;
H1 Collaboration, I. Abt et al., Nucl. Phys. **B 396** (1993) 3.

4 J. Blümlein and R. Rückl, Phys. Lett **B304** (1993) 337;
J. Blümlein and R. Rückl, in: Proc. of the Workshop on e^+e^- Collisions at 500 GeV: The Physics Potential, Munich, Annecy, Hamburg, 1991, ed. P.M. Zerwas, DESY 92-123B, p. 595.

5 D. Schaile and P.M. Zerwas, in: Proc. of the Workshop on Physics at Future Accelerators, La Thuile and Geneva, 1987, ed. J.H. Mulvey, CERN 87-07, Vol. II, p. 251;
A.Djouadi, M. Spira and P.M. Zerwas, in: Proc. of the Workshop on e^+e^- Collisions at 500 GeV: The Physics Potential, Munich, Annecy, Hamburg, 1991, ed. P.M. Zerwas, DESY 92-123B, p. 561;
J. L. Hewett and T.G. Rizzo, Phys. Rev. **D36** (1987) 3367.

6 D. Alexander et al., OPAL collaboration, Phys. Lett. **B275** (1992) 123;
D. Decamp et al., ALEPH collaboration, Phys. Rep. **216** (1992) 253;
O. Adriani, et al., L3 collaboration, Phys. Rep. **236** (1993) 1;
P. Abreu et al., DELPHI collaboration, Phys. Lett. **B316** (1993) 620.

7 J.L. Hewett and S. Pakvasa, Phys. Rev. **D37** (1988) 3165;
O.J.P. Éboli and A.V. Olinto, Phys. Rev. **D38** (1988) 3461;
M. de Montigny and L. Marleau, Phys. Rev. **D40** (1989) 2869; 3616; **D41** (1990) 3523; Can. J. Phys. **68** (1990) 612;
J.L. Hewett, T.G. Rizzo, S. Pakvasa, H.E. Haber, and A. Pomarol, in: Proc. of the Workshop on Physics at Current Accelerators and Supercolliders, Argonne, IL, June 1993, eds. J.L. Hewett,

A.R. White, and D. Zeppenfeld, (ANL, Argonne, 1993), p. 539;
J.E. Cieza-Montalvo and O.J.P. Éboli, Phys. Rev. **D50** (1994) 331.

8 J. Blümlein, E. Boos, and A. Kryukov, DESY report in preparation.

9 J. Blümlein, E. Boos, and A. Pukhov, DESY 94-072.

10 J. Blümlein and P.H. Frampton, in: Proc. of the Conference 'Physics and Experiments with Linear e^+e^- Colliders', Hawaii, April 1993, eds. F.A. Harris, S.L. Olsen, S. Pakvasa, and X. Tata, (World Scientific, Singapore, 1993) p. 926;
J. Blümlein, P.H. Frampton, and R. Rückl, in preparation.

11 W. Buchmüller, R. Rückl and D. Wyler, Phys. Lett. **B191** (1987) 442.

12 see e.g.: W. Beenakker, F. Berends and W. van Neerven, Proceedings of the Ringberg Workshop 'Radiative Corrections for e^+e^- Collisions', ed. J.H. Kühn, (Springer, Berlin, 1989), p. 3.

13 J. Blümlein, in: Proc. of the Conference 'Physics and Experiments with Linear e^+e^- Colliders', Hawaii, April 1993, eds. F.A. Harris, S.L. Olsen, S. Pakvasa, and X. Tata, (World Scientific, Singapore, 1993) p. 542;
J. Blümlein, in: Proc. of the Workshop on e^+e^- Collisions at 500 GeV: The Physics Potential, Munich, Annecy, Hamburg, 1993, ed. P.M. Zerwas, DESY 92-123C, p. 419;

14 J.E. Cieza-Montalvo and O.J.P. Éboli, Phys. Rev. **D47** (1993) 837.

15 J. Wudka, Phys. Lett. **B167** (1986) 337.

16 M. Bell and J.S. Bell, Part. Acc. **24** (1988) 1;
R. Blankenbecler and S.D. Drell, Phys. Rev. Lett. **61** (1988) 2324;
P. Chen and K. Yokoya, Phys. Rev. Lett. **61** (1988) 1101;
P. Chen, SLAC-PUB-5914;
P. Chen and S. Klein, SLAC-PUB-6021;
M. Jacob and T.T. Wu, Nucl. Phys. **B303** (1989) 389; Z. Phys. **C58** (1993) 279;
V.N. Baier, V.M. Katakov and V.M. Strakhovenko, Inst. Nucl. Phys. preprint, 88-168 (1988), Novosibirsk.

17 T. Barklow, P. Chen and W. Kozanecki, in: Proceedings of the Workshop 'e^+e^--Collisions at 500 GeV: The Physics Potential', ed. P.M. Zerwas, DESY 92-123B (DESY, Hamburg 1992), p. 845.

18 P. Igo-Kemenes, M. Martinez, R. Miquel, and S. Orteu, in: Proc. of the Workshop on e^+e^- Collisions at 500 GeV: The Physics Potential, Munich, Annecy, Hamburg, 1993, ed. P.M. Zerwas, DESY 92-123C, p. 319;

19 J. Schwinger, Particles, Sources and Fields, Vol. III (Addison-Wesley, Reading, MA, 1989), Ch. 5.4;
M. Drees and K. Hikasa, Phys. Lett. **B252** (1990) 127.

20 J.H. Kühn and P.M. Zerwas, Phys. Rep. **167** (1988) 321.

21 G. Bélanger, D. London, and H. Nadeau, in: Proc. of the Conference 'Physics and Experiments with Linear e^+e^- Colliders', Hawaii, April 1993, eds. F.A. Harris, S.L. Olsen, S. Pakvasa, and X. Tata, (World Scientific, Singapore, 1993) p. 538.

22 M.A. Doncheski and S. Godfrey, Phys. Rev. **D49** (1994) 6220.

23 I.F. Ginzburg, G.L. Kotkin, V.G. Serbo, and V.I. Telnov, Nucl. Inst. Meth. **205** (1983) 47.

24 J.L. Hewett and S. Pakvasa, Phys. Lett. **B227** (1989) 178.

25 H. Nadeau and D. London, Phys. Rev. **D47** (1993) 3742.

26 O.J.P. Éboli, E.M. Gregores, M.B. Magro, P.G. Mercadante, and S.F. Novaes, Phys. Lett. **B311** (1993) 147.

27 see e.g.: A.I. Akhiezer and V.B. Berestetskii, Quantum Electrodynamics, (Intersience, New York, 1965), Ch. IX and references therein.

28 S.Y. Choi and F. Schrempp, in: Proc. of the Workshop on e^+e^- Collisions at 500 GeV: The Physics Potential, Munich, Annecy, Hamburg, 1991, ed. P.M. Zerwas, DESY 92-123B, p. 793. Note a few misprints contained in Phys. Lett. **B272** (1991) 149.

29 F. Abe et al., CDF collaboration, Phys. Rev. **D48** (1993) R3939;
S. Abachi et al., D0 collaboration, Phys. Rev. Lett., **72** (1994) 965.

30 R. Rückl and P. Zerwas, in: Proc. of the Workshop on Physics at Future Accelerators, La Thuile and Geneva, 1987, ed. J.H. Mulvey, CERN 87-07, Vol. **II**, p. 220.

31 J. Ohnemus, S. Rudaz, T. Walsh, and P. Zerwas, DESY 94-086.